IEEE/CSC & ESAS European Superconductivity News Forum (ESNF), No. 6, October 2008
(ASC Preprint 3EA07 conforming to IEEE Policy on Electronic Dissemination, Section 8.1.9)
The published version of this manuscript appeared in *IEEE Transactions on Applied Superconductivity* **19**, No. 3, Part 1, 532 - 535 (2009)


# Noise Measurements in Hot-Electron Titanium Nanobolometers

Boris S. Karasik, Sergey V. Pereverzev, David Olaya, Jian Wei, Michael E. Gershenson, and Andrei V. Sergeev

***Abstract*—We are presenting experimental results on the electrical noise in small titanium hot-electron nanobolometers with the critical temperature above 300 mK. The noise data demonstrate good agreement with the conventional bolometer theory prediction. The noise is dominated by the thermal energy fluctuations (phonon noise) when the operating temperature is set just a few mK below the superconducting transition. The corresponding noise equivalent power (*NEP*) is about $3\times10^{-18}$ W/Hz$^{1/2}$ for the smallest measured device. The relative NEP's for the two devices measured scale roughly as the square root of the device volume as one would expect from the theory. Therefore an additional factor of 2-3 reduction of *NEP* may be feasible if the length and width of our device are further reduced. The demonstrated combination of the low NEP and the relatively high operating temperature is attractive for submillimeter low-background applications.**

***Index Terms*—bolometers, superconducting device noise, submillimeter wave detectors, superconducting radiation detectors.**

## I. INTRODUCTION

RECENT demonstration of an extremely low thermal conductance in titanium (Ti) hot-electron superconducting nanobolometers [1,2] has proven the early predictions [3] for this detector type. The lowest achieved thermal conductance due to the electron-phonon decoupling in Ti nanodevices with niobium (Nb) Andreev contacts (~ 100 fW/K at 300 mK and ~ 0.1 fW/K at 40 mK, see Fig. 1) translates into the "phonon-noise" *NEP* ≈ $3\times10^{-21}$ W/Hz$^{1/2}$ at 40 mK and *NEP* ≈ $7\times10^{-19}$ W/Hz$^{1/2}$ at 300 mK. Such a low *NEP* is required for the recently proposed advanced space submillimeter astrophysics missions (SAFIR [4], SPECS [5], SPICA [6]) where the active cooling of the telescope primary mirror down to ~ 4 K would practically eliminate the mirror thermal emission. Under such conditions, the background-limited *NEP* for the moderate resolution spectroscopy ($\nu/\delta\nu$ ~ 1000; corresponds to a typical width of a Doppler-broadened extragalactic emission spectral line) would be $10^{-19}$-$10^{-20}$ W/Hz$^{1/2}$ across the submillimeter wavelength range. A more moderate (*NEP* ~ $10^{-18}$ W/Hz$^{1/2}$) sensitivity is needed for photometric and polarimetric applications in space ($\nu/\delta\nu$ ~ 4).

The electron-phonon thermal conductance achieved in nanobolometers ($G_{e\text{-}ph}$) below 300 mK turns out to be significantly lower than the thermal conductance due to the phonon transport in the best Si-N membrane supported bolometers (e.g., [7], see Fig. 1). However, the actual *NEP* measurements have not been done yet in hot-electron nanobolometers. In the current work, we demonstrate that the electrical noise in the improved devices with the critical temperature $T_C$ = 330-360 mK is well explained by the conventional noise mechanism associated with the fluctuations of electron thermal energy in the device. The contributions of the Johnson noise and the readout noise have been found to be negligible compared to the phonon noise.

## II. DEVICES AND EXPERIMENTAL SETUP

The small devices described in [1] had rather low $T_C$ values, that was likely the result of contamination of Ti material during e-beam evaporation of Ti through an organic mask (see [1] for fabrication details). The critical current in the

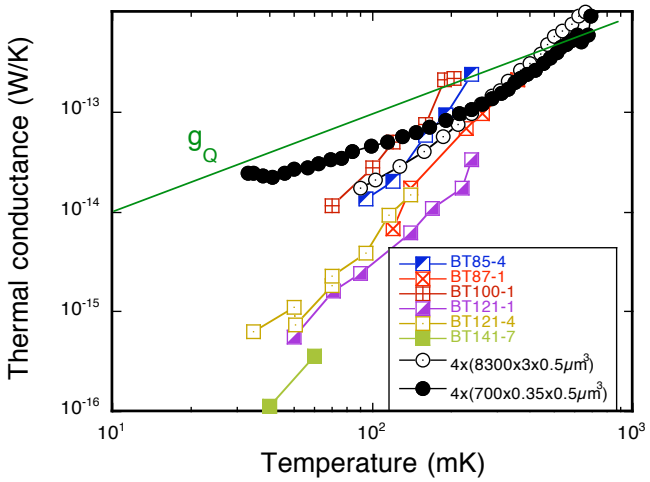


Fig.1. Comparison of the thermal conductance in $Si_3N_4$ beam suspended bolometers [7] (round symbols) and in Ti hot-electron nanobolometers similar to those described in [1] (square symbols). The Ti devices were 40 nm thick, 0.1-0.14 μm wide and 0.5-1.0 μm long. $g_Q = \pi^2 k_B^2 T/3h$ is the so-called "quantum of thermal conductance" which is the limit of the thermal conductance for 1D photons and 1D ballistic phonons.

Manuscript received 26 August 2008. The research described in this paper was carried out at the Jet Propulsion Laboratory, California Institute of Technology, under a contract with the National Aeronautics and Space Administration.

B. S. Karasik and S. V. Pereverzev are with the Jet Propulsion Laboratory, California Institute of Technology, Pasadena, CA 91109 (BSK's phone: 818-393-4438; fax: 818-393-4683; e-mail: boris.s.karasik@jpl.nasa.gov).

D. Olaya was with Rutgers University, Piscataway, NJ 08854 USA. He is now with the National Institute of Standards and Technology, Boulder, CO 80305 (email: david.olaya@nist.gov).

J. Wei was with Rutgers University, Piscataway, NJ 08854 USA. He is now with Northwestern University, Evanston, IL 60208 (email: jian-wei@northwestern.edu).

M. E. Gershenson is with Rutgers University, Piscataway, NJ 08854, USA (gersh@physics.rutgers.edu)

A. V. Sergeev is with State University of New York at Buffalo, Buffalo, NY 14260 (email: asergeev@eng.buffalo.edu).

devices was also small. In order to avoid this deterioration of superconducting parameters we fabricated somewhat larger devices from a thicker (60 nm) Ti film on Si substrates. The same as in [1] process was used for *in situ* deposition of Ti bridges and Nb Andreev contacts. In this work, we studied two devices of different size whose parameters are presented in Table I.

TABLE I PARAMETERS OF TI NANOBOLOMETERS

| Device | Length (μm) | Width ($\mu$m) | $T_C$ (mK) | $R_N$ (Ohm) | $G$ (pW/K) |
|---|---|---|---|---|---|
| 1 | 6 | 0.4 | 330 | 55 | 7-8 |
| 2 | 2 | 0.15 | 355 | 70 | 1-2 |

$R_N$ is the device normal resistance.

The devices were tested in a dilution refrigerator. A constant dc bias current was passed though a 1-Ohm resistor situated in the vicinity of the device on the mixing chamber. This resistor was connected in series with the device and with the dc SQUID thus creating the constant voltage bias. The SQUID amplifier was placed at the 1-K pot of the dilution refrigerator and connected to the device circuit via a magnetically shielded superconducting twisted pair. The device circuit was in an rf tight superconducting shield in order to avoid overheating of the device by uncontrolled rf interferences and noise. The entire experimental volume was surrounded by a Cryoperm-10® magnetic shield immersed in liquid He4. The bias lines and the SQUID wires were fed through custom low-pass filters (LPF), which were built from discrete element LPFs placed inside metal tubes filled with Emerson&Cuming CRS-124 microwave absorbing compound. This approach was inspired by a recent work [8].

## III. CURRENT-VOLTAGE CHARACTERISTICS AND ELECTRICAL NOISE

A family of the current-voltage (IV) characteristics for device #1 is shown in Fig. 2 as function of temperature. The device normal resistance, $R_N$, was 55 Ohm and the residual resistance was much less than 1 Ohm. The critical current is very pronounced below $T_C$ (≈ 330 mK) but quickly collapses as the temperature increases by a few mK. Because of the dc stability condition $|dV/dI| > R_L$ ($R_L$ is the load resistance), it was not possible to obtain a complete (continuous) IV characteristic without switching for this device below 323 mK.

We used the so-called "isothermal" technique [9,10], which has been commonly used in superconducting hot-electron heterodyne detectors, to measure the thermal conductance in both devices of Table I. In this technique, an assumption is made that the bolometer resistance is function of the electron temperature only and, thus, the constant resistance lines are the electron temperature isotherms. Then if one takes a difference of any two Joule power values (e.g., $P1$ and $P2$) dissipated in two crosspoints (1 and 2, see Fig. 2) of an $R$ = const line (isotherm) with two IV characteristics taken at slightly different bath temperatures (e.g., at $T1$ = 323 mK and at $T2$ = 325 mK in Fig. 2), the thermal conductance $G$ can be found as

$$G = \frac{P1 - P2}{T2 - T1}. \quad (1)$$

Using this approach, the $G$ values of Table I have been found. For device #1, $G \approx$ 7-8 pW/K is in good agreement with the $G_{e\text{-}ph}$ data of [1], which can be approximated above 0.3 K by the following expression:

$$G_{e-ph}(T) = 1.56 \times 10^9 T^3 \Omega \quad [\text{W/K}]. \quad (2)$$

Here $\Omega$ is the device volume in m$^3$.

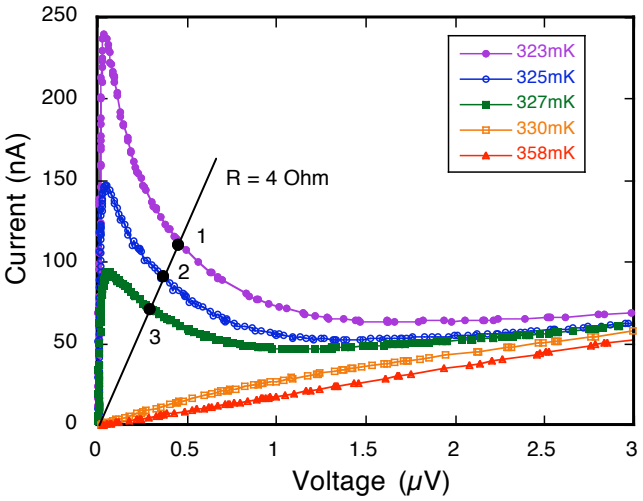


Fig. 2. IV characteristics for device #1. The load resistance of an equivalent voltage source was 1 Ohm. A constant resistance line ($R$ = 4 Ohm) is shown to illustrate the "isothermal" technique used for determination of the thermal conductance.

Figure 3 shows the electrical (current) noise in device #1 measured at 3 kHz as function of bias at 325 mK. The maximum noise values ~40 pA/Hz$^{1/2}$ was observed at low bias voltages. The noise gradually decreases with bias. This is easy to understand qualitatively since the responsivity of a voltage-bias bolometer (and its phonon noise) gets higher towards the low bias values. The maximum noise far exceeds the SQUID noise (2.2 pA/Hz$^{1/2}$).

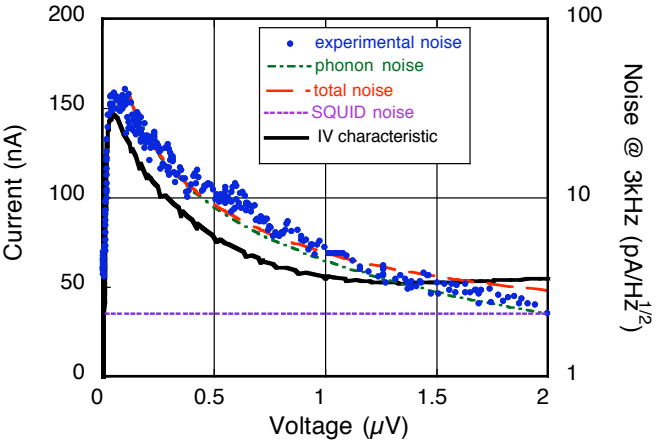


Fig.3. IV characteristic and electrical noise of device #1 at 325 mK. The results of modeling show that the phonon noise dominates if the bias voltage is less than 1 μV.

The noise spectrum at the bias point corresponding to the maximum noise is shown in Fig. 4. In general, the noise spectrum is flat, though there is a slight increase of the noise towards lower frequencies below 1 kHz. This increase is absent in the SQUID noise (bottom curve) and in the Johnson noise of a 1-Ohm load resistor (middle curve). The origin of this noise is not known yet.

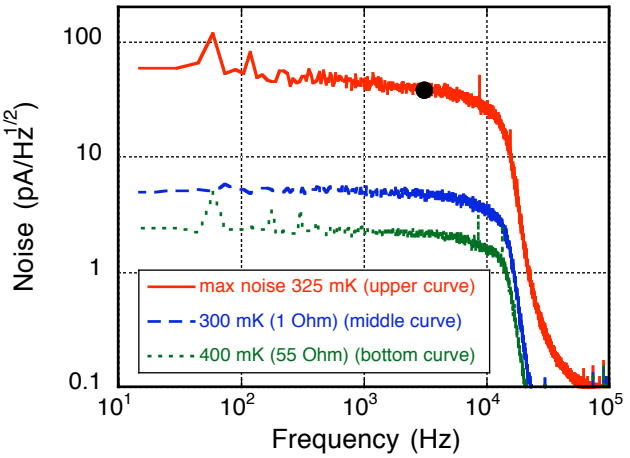


Fig. 4. Noise spectrum of device #1 at 325 mK. The dot indicates the frequency (3 kHz) at which the data of Fig. 3 were taken. Noise spectra of the device in the superconducting state (300 mK, no bias) and in the normal state (400 mK) are also shown. The roll-off at 15 kHz is due to the filter in the SQUID feedback loop and a room temperature 7-pole LPF used in the experiment.

The roll-off of the noise spectrum was a result of a combined effect of the SQUID feedback loop filter and of a room temperature 7-pole low-pass filter. The phonon noise should roll-off at the frequency corresponding to the device thermal relaxation time. At this temperature, this would be above 80 kHz (see below) and could not be seen in the data of Fig. 4.

In order to get a better idea about the origin of the device noise we calculated the output noise using the model for a lumped element bolometer developed in [11-14]. In this model, the negative electro-thermal feedback (ETF) plays an important role modifying the output noise and the thermal relaxation time. The dimensionless parameter characterizing the feedback (the loop gain, $L$) was derived from the IV characteristics using the expression:

$$L = \frac{dV/dI + V/I}{dV/dI - V/I} \qquad (3)$$

($V$ is the bias voltage and $I$ is the bias current).

We found that the part of the IV curve below 200 nV (where the responsivity is greater) can be approximated as $I \sim 1/V^m$. The extreme theoretical case $m$ = 1 (strong negative ETF) has been considered, e.g., in [10]. In was not the case in our measurements where we obtained $m \approx 0.37$. The loop gain relates to exponent $m$:

$$L = \frac{1+m}{1-m} \qquad (4)$$

yielding $L$ = 2.2 at 325 mK. Using this value, the phonon noise and the Johnson noise have been calculated:

$$i_n^{phon} = \frac{\sqrt{4k_B T^2 G_{e-ph}}}{V}\frac{L}{1+L}, \qquad i_n^J = \sqrt{\frac{4k_B T}{R(1+L)}}. \qquad (5)$$

The results of calculations of the phonon noise contribution and also of the total noise are plotted in Fig. 3. One can see that the total noise agrees very well with the experimental values. The modeling suggests that the phonon noise dominates and two other noise components (SQUID noise and Johnson noise) are negligibly small. This is an indication that the intrinsic responsivity in the bias points below 200 nV is sufficiently high (it nearly reaches $1\times10^7$ A/W), and that the total *NEP* can be estimated using the well-known expression:

$$NEP = \sqrt{4k_B T^2 G_{e-ph}} = (6\text{-}7)\times10^{-18}\ \mathrm{W/Hz^{1/2}}. \qquad (6)$$

The bolometer "bare" time constant $C_e/G_{e\text{-}ph} \approx 2$ μs but the actual bolometer response time is modified by the ETF and can be found as

$$\tau = \frac{C_e/G_{e-ph}}{1+L} \approx 0.6\ \mu\mathrm{s}. \qquad (7)$$

(we used bulk Sommerfeld constant value $\gamma = 310$ J m$^{-3}$ K$^{-2}$ for Ti).

A smaller device #2 demonstrated similar tendencies, though the IV characteristics for this device were not as smooth as for device #1 (see Fig. 5). This might be due to the extremely small device width which gives rise to some granulation and non-uniformity of the critical temperature and the critical current density along the device. Because of that, the value of the thermal conductance $G$ could not be estimated uniformly using Eq. 1 for an arbitrary $R$ = const line and varied within a factor of 2 ($G$ = 1-2 pW/K). This value still agrees reasonably well with the prediction of Eq. 2.

The behavior of the device noise with bias was similar to that of device #1. In the example of Fig. 5, the maximum noise was about 100 pA/Hz$^{1/2}$, and parameter $m$ derived from the IV curve was about 0.8. Thus, the maximum noise expected from

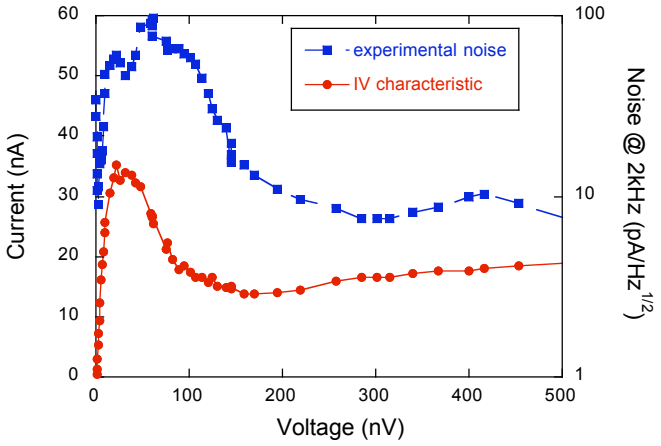


Fig.5. IV characteristic and electrical noise in device #2 at 350 mK.

the theory was 70 pA/Hz$^{1/2}$. Given the uncertainty in the value of $G$, the estimated $NEP$ is (2-4)×10$^{-18}$ W/Hz$^{1/2}$ at 350 mK.

The electro-thermal feedback loop parameter was very large for device #2 ($L$ = 9), so the time constant should be close to 0.1 μs. It is interesting to note that the found time constants are significantly shorter than the electrical time constant of the circuit $\tau_{el} = L_{SQUID}/(R+R_L)$. The SQUID input coil inductance was $L_{SQUID}$ = 1.8 μH and the device resistance was well under 1 Ohm for small bias voltages. Still the operating point was stable in the region where $dV/dI < 0$. Previous analytical papers [15,16] derived a more conservative stability condition: $\tau > (3\text{-}6) \times \tau_{el}$.

## IV. Conclusion

The obtained results demonstrate a very good potential of the hot-electron bolometers for becoming an attractive detector technology in low background submillimeter applications. Although more technological work is needed in order to improve the quality of the smallest devices (devices as small as 0.6μm × 0.1μm × 0.04μm were used in [1]), the larger devices studied in this work have already sufficiently good characteristics having reached the noise limit set by the fundamental thermal energy fluctuations. The next step would be to perform optical *NEP* measurements with similar devices integrated with planar antennas. The device normal resistance of about 50 Ohm is a perfect match for typical planar antenna impedances.

An electrical $NEP < 10^{-17}$ W/Hz$^{1/2}$ achieved at $T > 300$ mK sets the record for this temperature. Other types of detectors may be that sensitive only a temperatures 50-100 mK. Temperatures higher than 300 mK can be readily achieved using sorption coolers, which are simple and inexpensive. The very short detector time constant is instrumental for eliminating the 1/f-noise and increasing the data rate from the instrument.

## Acknowledgment

B.S. Karasik thanks D. Santavicca and D.E. Prober for receiving a manuscript of their paper [8] before publication.

## References

[1] J. Wei, D. Olaya, B.S. Karasik, S.V. Pereverzev, A.V. Sergeev, and M.E. Gershenson, "Ultra-sensitive hot-electron nanobolometers for terahertz astrophysics", *Nature Nanotechnol.*, vol.3, pp. 496-500, Aug. 2008.

[2] B.S. Karasik, D. Olaya, J. Wei, S. Pereverzev, M.E. Gershenson, J.H. Kawamura, W.R. McGrath, and A.V. Sergeev, "Record low NEP in the hot-electron titanium nanobolometers," *IEEE Trans. Appl. Supercond.*, vol. 17, pp. 293-297, Jun. 2007.

[3] B.S. Karasik, W.R. McGrath, H.G. LeDuc, and M.E. Gershenson, "A hot-electron direct detector for radioastronomy," *Supercond.: Sci. & Technol.*, vol. 12, pp. 745-747, Nov. 1999; B.S. Karasik, W.R. McGrath, M.E. Gershenson, and A.V. Sergeev, "Photon-noise-limited direct detector based on disorder-controlled electron heating," *J. Appl. Phys.*, vol.87, pp.7586-7588, May 2000.

[4] D.J. Benford and S.H. Moseley, "Cryogenic detectors for infrared astronomy: the Single Aperture Far-InfraRed (SAFIR) Observatory," *Nucl. Instr. Meth. Phys. Res. A,* vol. 520, pp. 379-383, Mar. 2004.

[5] D. Leisawitz, "NASA's far-IR/submillimeter roadmap missions: SAFIR and SPECS," *Adv. Space Res.,* vol. 34, pp. 631-636 (2004).

[6] T. Nakagawa, "SPICA: space infrared telescope for cosmology and astrophysics," *Adv. Space Res.,* vol. 34, pp. 645-650 (2004).

[7] M. Kenyon, P.K. Day, C.M. Bradford, J.J. Bock, and H.G. Leduc, "Progress on background-limited membrane-isolated TES bolometers for far-IR/submillimeter spectroscopy," *Proc. SPIE*, vol. 6275, 627508 (2006).

[8] D.F. Santavicca and D.E. Prober, "Impedance-matched low-pass stripline filters," *Meas. Sci. Technol.*, vol. 19, 087001, Aug. 2008.

[9] E.M. Gershenzon, G.N. Gol'tsman, A.I. Elant'ev, B.S. Karasik, and S.E.Potoskuev, "Intense electromagnetic radiation heating of electrons of a superconductor in the resistive state," *Fiz. Nizk. Temp.*, vol. 14, pp. 753-763, Jul. 1988 [*Sov. J. Low Temp. Phys.,* vol. 14, pp. 414-420 (1988)].

[10] A.I. Elantev and B.S. Karasik, "Effect of high frequency current on Nb superconductive film in the resistive state," *Fiz.Nizk.Temp.,* vol. 15, pp. 675-683, Jul. 1989 [*Sov. J. Low Temp. Phys.,* vol. 15, pp. 379-383 (1989)].

[11] J.C. Mather, "Bolometer noise: nonequilibrium theory," *Appl. Opt.,* vol. 21, pp. 1125-1129, Mar. 1982.

[12] K.D. Irwin, "An application of electrothermal feedback for high resolution cryogenic particle detection," *Appl. Phys. Lett.*, vol. 66, pp. 1998-2000, Apr. 1995.

[13] B.S. Karasik and A.I. Elantev, "Noise temperature of a superconducting hot-electron mixer," in *Proc. 6th Int. Symp. Space Terahertz Technol.,* Pasadena, California, 1995, pp. 229-246.

[14] B.S. Karasik and A.V. Elantiev, "Noise temperature limit of a superconducting hot electron bolometer mixer," *Appl. Phys. Lett.*, vol. 68, pp. 853-855, Feb. 1996.

[15] K.D. Irwin, G.C. Hilton, D.A. Wollman, and J.M. Martinis, "Thermal-response time of superconducting transition-edge microcalorimeters," *J. Appl. Phys.*, vol. 83, pp. 3978-3985, Apr. 1998.

[16] W.A. Mels, M.P. Bruijn, H.F.C. Hoevers, M. Frericks, F.B. Kiewiet, A.C. Bento, and P.A.J. de Korte, "Performance of hot-electron bolometers for infrared and X-ray detection," in *Proc. SPIE*, vol. 3445, pp. 255-265 (1998).